

# Exploiting Constructive Interference for Scalable Flooding in Wireless Networks

Yin Wang, *Member, IEEE*, Yuan He, *Member, IEEE*, Xufei Mao, *Member, IEEE*, Yunhao Liu, *Senior Member, IEEE*, and Xiang-yang Li, *Senior Member, IEEE*

**Abstract**—Constructive interference-based flooding (CIBF) is a latency-optimal flooding protocol, which can realize millisecond network flooding latency and submicrosecond time synchronization accuracy, require no network state information, and be adapted to topology changes. However, constructive interference (CI) has a precondition to function, i.e., the maximum temporal displacement  $\Delta$  of concurrent packet transmissions should be less than a given hardware constrained threshold (e.g.,  $0.5 \mu\text{s}$ , for the IEEE 802.15.4 radio). In this paper, we derive the closed-form packet reception ratio (PRR) formula for CIBF and theoretically disclose that CIBF suffers the scalability problem. The packet reception performance of intermediate nodes degrades significantly as the density or the size of the network increases. We analytically show that CIBF has a PRR lower bound (94.5%) in the grid topology. Based on this observation, we propose the spine constructive interference-based flooding (SCIF) protocol for an arbitrary uniformly distributed topology. Extensive simulations show that SCIF floods the entire network much more reliably than the state-of-the-art Glossy protocol does in high-density or large-scale networks. We further explain the root cause of CI with waveform analysis, which is mainly examined in simulations and experiments.

**Index Terms**—Concurrent transmissions, constructive interference (CI), network flooding, topology control, wireless networks.

## I. INTRODUCTION

NETWORK flooding is a fundamental service in wireless ad hoc networks for many purposes, such as data dissemination [1], time synchronization [2], the creation of a data collection tree [3], etc. The main objective of network flooding

Manuscript received June 29, 2012; revised November 07, 2012; accepted December 10, 2012; approved by IEEE/ACM TRANSACTIONS ON NETWORKING Editor S. Chen. Date of publication January 29, 2013; date of current version December 13, 2013. This work was supported by the NSFC under Grants Major No. 61190110, Distinguished Young Scholars No. 61125202, No. 61170213, No. 61170216, No. 61228202, and No. 61272426; the NSF under Grants CNS-0832120, CNS-1035894, and ECCS-1247944; the China Postdoctoral Science Foundation under Grants No. 2011M500019, No. 2012T50096, and No. 2012M510029; China 973 under Grants No. 2012CB316200 and No. 2011CB302705; China 863 under Grant No. 2011AA010100; and the Science and Technology on Communication Information Security Control Laboratory, China.

Y. Wang, Y. He, and X. Mao are with the TNLIST, School of Software, Tsinghua University, Beijing 100084, China (e-mail: yin-wang10@mails.tsinghua.edu.cn; he@greenorbs.com; xufei.mao@gmail.com).

Y. Liu is with the TNLIST, School of Software, Tsinghua University, Beijing 100084, China, and also with the Department of Computer Science and Engineering, Hong Kong University of Science and Technology (HKUST), Hong Kong (e-mail: yunhao@greenorbs.com).

X.-Y. Li is with the Department of Computer Science, Illinois Institute of Technology, Chicago, IL 60616 USA (e-mail: xli@cs.iit.edu).

Color versions of one or more of the figures in this paper are available online at <http://ieeexplore.ieee.org>.

Digital Object Identifier 10.1109/TNET.2013.2238951

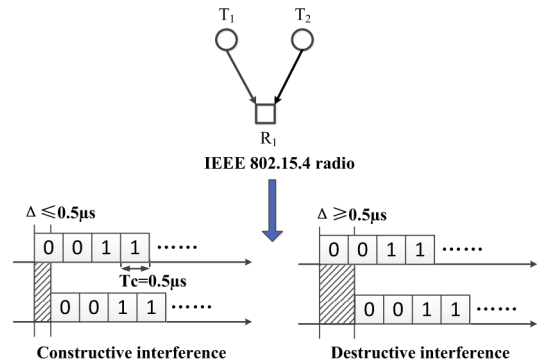


Fig. 1. Concurrent transmissions of an identical packet with the IEEE 802.15.4 radio.

is to propagate packets reliably and as fast as possible. By leveraging link characteristics such as link correlation [4], link dynamics [5], and link quality [6], current approaches focus on identifying which nodes to relay packets. Unfortunately, those approaches suffer high overhead to maintain the network state. By exploring properties of wireless radios such as the capture effect [7] and implementing controlled concurrency, Flash [8] achieves rapid network flooding with 2 s latency for 90% reliability in a network consisting of 48 Tmote Sky motes. Glossy [9] achieves a magnitude of millisecond flooding latency and submicrosecond per-hop time synchronization accuracy and is the fastest packet propagation protocol known in the literature. Glossy employs a concurrent transmission technique called constructive interference (CI) [10]. Interference is constructive if it *helps* the common receiver to decode the original signal. By contrast, interference is destructive if it *prevents* the common receiver from accurately decoding the superimposed signals, as illustrated in Fig. 1.

Recently employed in Backcast [10], CI can alleviate the ACK storm problem [11], reduce the transmission latency of acknowledge packets, and improve the reliability of packet transmissions [12]. CI originates from the physical layer tolerance for multipath signals: When multiple senders transmit an identical packet simultaneously, concurrent packet transmissions can improve the packet reception rate (PRR) of a common receiver, rather than causing mutual interference. However, CI has a precondition that requires the maximum temporal displacement  $\Delta$  of concurrent packet transmissions should be no more than a threshold duration, which is constrained by physical-layer designs and equals to  $0.5 \mu\text{s}$  for IEEE 802.15.4 compatible receivers.

The phenomena of CI is previously examined in simulations [9] and experiments [10]. In this paper, we explore the root

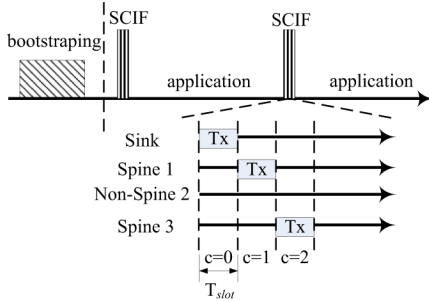


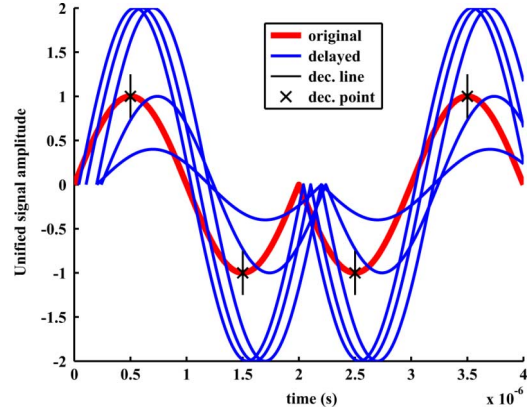
Fig. 2. SCIF temporally decouples with application tasks.

cause of CI with waveform analysis, derive the closed-form formula to calculate PRR performance in the worst-case topology, and theoretically disclose that constructive interference-based flooding (CIBF) suffers the scalability problem. Namely, PRR decreases significantly when the density (defined as the number of nodes in a unit area) or the size (defined as the maximum hops of the shortest path between any two nodes) of the network grows. We show that a network with a grid topology can efficiently resist packet collisions induced by scalable flooding. Based on this observation, we further propose the spine constructive interference-based flooding (SCIF) protocol for the network with a general topology, which first constructs the spine of a given topology, and then conducts network flooding on the spine following the main idea of Glossy. The key difference is that the dominatee nodes connecting to the spine only receive the flooding packets, rather than retransmitting those packets. Extensive simulations show that the PRR of SCIF is much higher than that of Glossy in high density and large-scale wireless networks. It is worth mentioning that we take IEEE 802.15.4 radio as an example in this discussion, and the analysis can be easily extended to other radios.

With an elaborate cross-layer design, SCIF temporally decouples network flooding from upper-layer application tasks, as shown in Fig. 2. During the period of SCIF, synchronized nodes receive and forward packets according to strictly assigned time-slots, performing packet transmissions in a highly predictable way, rather than leveraging traditional CSMA/CA protocols.

The major contributions are summarized as follows.

- 1) We show the root cause of CI with waveform analysis. Moreover, we derive the closed-form PRR formula, which not only considers the power constraint due to signal-to-noise ratio, but also includes the phase constraint with respect to the probability that CI satisfies its precondition.
- 2) To the best of our knowledge, this is the first work to theoretically and experimentally disclose the scalability problem of CIBF. Moreover, we theoretically prove that the PRR of CIBF has a lower bound (94.5%) even if the network scales, which is also validated by extensive simulations.
- 3) The PRR performance of SCIF protocol outperforms that of Glossy by constructing a virtual backbone of a given topology. For instance, simulations show that the PRR of SCIF keeps stable above 96% as the network size grows from 400 to 4000, while the PRR of Glossy is only 26% when the network size is 4000.

Fig. 3. Constructive interference (time displacement  $\Delta \leq T_c$ ).TABLE I  
SYMBOLS AND NOTATIONS

Symbol	Definition
$\Pi_R$	signal noise ratio gain of the received signals due to CI
$\text{PRR}_{\text{Link}}$	PRR due to unreliable wireless links
$T_{\text{slot}}$	duration of the two start instants for adjacent transmissions
$c$	relay counter, increase by 1 after each retransmission
$N$	maximum number of times a node transmit during a flood
$\text{PRR}_{\text{R1}}^{\text{Topo}}$	PRR of R1 due to unsynchronized transmissions
$\text{PRR}_{\text{R1}}$	The aggregate received PRR of R1

The rest of this paper is organized as follows. Section II presents the waveform analysis of CI for IEEE 802.15.4 radio. Section III introduces the radio triggered synchronization mechanism and timing diagram of CIBF and reveals the scalability problem, followed by the design of the SCIF protocol in Section IV. Section V presents the simulation results. Section VI discusses the related work. We conclude the work in Section VII.

## II. THEORETICAL ANALYSIS OF CONSTRUCTIVE INTERFERENCE

For ease of presentation, Table I lists the main symbols and notations used in this paper. Fig. 3 shows a 4-chips  $([1 \ 0 \ 0 \ 1])$  MSK signal with five replicas, received by a common IEEE 802.15.4 compatible receiver. For simplicity, the original signal is assumed to have unit amplitude and zero phase offset. Amplitudes and phase offsets of the five replicas are uniformly distributed in  $[0, 2]$  and  $[0, 0.5]$   $\mu\text{s}$ , respectively. It can be observed from Fig. 3 that the original signal has the same signs as the five replicas at critical time  $(2n+1)T_c$  ( $n = 0, 1, 2, \dots$ ). Interestingly, rather than resulting in mutual interference, the five replicas *help* the receiver decode the original signal. Meanwhile in Fig. 4, when the maximum temporal displacement  $\Delta$  among those transmitted signals exceeds one chip period  $T_c$  ( $0.5 \mu\text{s}$ ), the five replicas might have opposite signs with the expected signal at those critical decision time, leading to signal overlapping.

The basic principle of the 802.15.4 PHY layer is elaborated in [13]. Let  $S_{\text{msk}}(t)$  be the transmitted signal after MSK modulation, and  $I(t)$  and  $Q(t)$  denote the in-phase component and quadrature-phase component, respectively. Let  $\omega_c = \pi/2T_c$

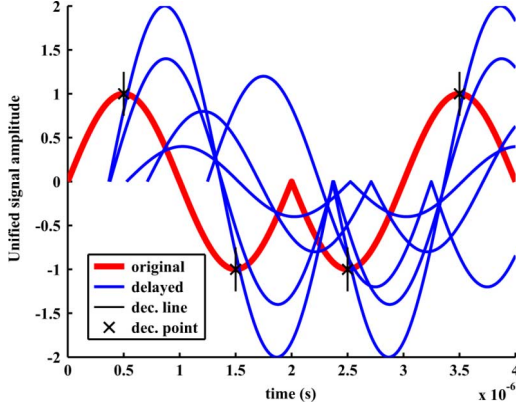


Fig. 4. Destructive interference (time displacement  $\Delta > T_c$ ).

represent the radial frequency of half-sine pulse shaping. The combined MSK signal can be calculated as

$$S_{\text{msk}}(t) = I(t) \sin \omega_c t - Q(t) \cos \omega_c t \quad (1)$$

where

$$\begin{cases} I(t) = \sum_n (2C_{2n} - 1) \text{rect}(\frac{t}{2} - nT_c) \\ Q(t) = \sum_n (2C_{2n+1} - 1) \text{rect}(\frac{t}{2} - nT_c - \frac{T_c}{2}). \end{cases} \quad (2)$$

Here,  $C_n \in \{0, 1\}$  represents the  $n$ th chip, and  $\text{rect}(t)$  function is defined as the rectangle window ranging from 0 to  $T_c$ . Assuming the Gaussian flat fading channel,<sup>1</sup> we obtain the received signal  $S_R(t)$

$$S_R(t) = \sum_{i=0}^K A_i S_{\text{msk}}(t - \tau_i) + N_i(t) \quad (3)$$

where  $A_i$  and  $\tau_i$  depict the amplitude and phase offset of the  $i$ th transmitted signal, respectively,  $N_i(t)$  denotes the additional Gaussian white noise. The demodulated in-phase component of the received signal  $I_R(t)$  at decision time  $(2n + 1)T_c$  is

$$I_R(t)|_{t=(2n+1)T_c} = (2C_{2n} - 1) \sum_{i=0}^K A_i \cos \omega_c \tau_i + (-1)^n N((2n + 1)T_c) \quad (0 \leq \tau_i \leq T_c). \quad (4)$$

Similarly, the orthogonal-phase component of the receiving signal  $Q_R(t)$  at the decision time  $(2n + 2)T_c$  is

$$Q_R(t)|_{t=(2n+2)T_c} = (2C_{2n+1} - 1) \sum_{i=0}^K A_i \cos \omega_c \tau_i + (-1)^{(n+1)} N((2n + 2)T_c) \quad (0 \leq \tau_i \leq T_c). \quad (5)$$

Equations (4) and (5) indicate that if delayed offsets of  $K$  replicas are less than one chip period  $T_c$ , the demodulated chips are exactly the same as the transmitted chips. However, if the delayed offsets do not satisfy the above constraints, delayed replicas will interfere with the original signal, influence demodulating the in-phase or the orthogonal-phase component, and hence bring bit errors. The results obtained by theoretical

<sup>1</sup>Similar analysis can be extended to a more general Rayleigh fading multipath channel.

analysis in (4) and (5) match those of waveform analysis observed in Figs. 3 and 4. The above results disclose the root cause of the precondition of CI.

In order to quantitatively measure the improved reception performance due to CI, we define IGF  $\Pi_R$  as the improved signal-to-noise ratio (SNR) of the received signals.  $\Pi_R$  can be obtained from (3)–(5)

$$\Pi_R = \left( \frac{\sum_{i=0}^K A_i \cos \omega_c \tau_i^2}{K + 1} \right). \quad (6)$$

Equation (6) indicates that CI brings a  $K$ -fold improvement in the received SNR of  $K$  combined signals, when they are perfectly aligned. According to [13], the bit error rate (BER) of the received superposed signal is given by

$$P_e = Q\left(\sqrt{2\Pi_R \frac{S}{N}}\right) \quad (7)$$

where  $\frac{S}{N}$  represents the received SNR of a single transmitted signal and the  $Q$  function is the tail probability of the standard normal distribution [13]. Remembering that the 16 hamming mapping sequences of the IEEE 802.15.4 radio can correct eight bit errors of demodulated bit streams, hence, given BER, symbol error rate (SER) could be calculated as

$$P_s = \sum_{i=9}^{32} C(32, i) (1 - P_e)^{32-i} P_e^i. \quad (8)$$

For a packet with a length of  $l$  symbols, PRR due to link quality could be derived from (8)

$$\text{PRR}^{\text{Link}} = 1 - (1 - P_s)^l \quad (9)$$

where  $\text{PRR}^{\text{Link}}$  describes link-layer behaviors of receivers on condition of CI. The simulation validation of closed-form (9) is given in Section V-A.

### III. CONSTRUCTIVE INTERFERENCE-BASED FLOODING AND THE SCALABILITY PROBLEM

#### A. Radio Triggered Synchronization Mechanism

Traditionally, to propagate a packet across the entire network, intermediate nodes use CSMA/CA protocol to avoid potential packet collisions [4], [8]. However, due to carrier-sense phenomena and intrinsic disadvantages of the random backoff mechanism, the protocol results in high network flooding latency, which is usually much more serious in high-density and large-scale networks. CBIF schemes (e.g., Glossy), make simultaneous transmissions of packets with the same contents interfere constructively. In Glossy, intermediate nodes forward overheard packets immediately after receiving them. This triggers more nodes to receive the packets simultaneously, and the latter also start to relay the same packets concurrently. By taking considerable care to transmit data packets with precise timing, Glossy exploits CI by quickly propagating a packet from the sink node to all the other nodes across the entire network. In this way, Glossy reaches near-optimal flooding latency (see Lemma 3.1).

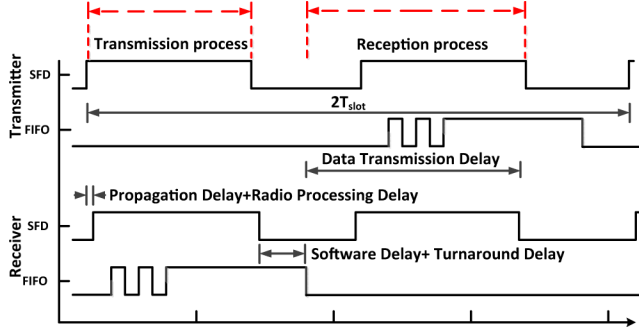


Fig. 5. Pin activities of CIBF captured by Agilent oscilloscope MSO-X 2024A.

*Lemma 3.1:* CIBF is a nearly latency-optimal protocol in multihop wireless networks.

The proofs of Lemmas 3.1, 3.2 (see Section III-B), 4.1, 4.2, and 4.3 (see Section IV-A) are provided in the extended version of this paper [14].

However, in practice, it is difficult to keep precise timing for concurrent packet transmissions in distributed systems. One straightforward approach is through accurate time synchronization. However, it is very challenging to realize 0.5- $\mu$ s time synchronization accuracy especially in multihop ad hoc wireless networks. To the best of our knowledge, the state-of-the-art time synchronization protocols [2] cannot approach such a time synchronization accuracy in multihop scenarios. CIBF is a radio triggered synchronization protocol, which leverages the instant of a broadcast packet as a common reference for all receivers to implement synchronized retransmissions. Through elaborate timing control, CIBF that enables the maximal temporal displacement  $\Delta$  of multiple concurrent transmissions satisfies the precondition of CI, i.e., the 0.5  $\mu$ s constraint.

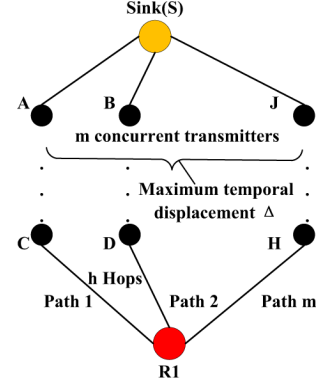
### B. Scalability Problem

In this section, we analyze the performance of CIBF in multihop scenarios. We define the minimum duration of the periodical SFD signal as a time-slot  $T_{\text{slot}}$ , which accounts for the time between the start of a packet transmission with relay counter  $c$  and the start of the following packet transmission with relay counter  $c + 1$ . Fig. 5 illustrates the detailed pin activities during packet reception and retransmission between a transmitter and a receiver. From Fig. 5, it can be observed that  $T_{\text{slot}}$  accounts for the software delay  $T_{\text{sw}}$ , the radio processing delay  $T_{\text{d}}$  introduced by the radio at the beginning of a packet reception, the propagation delay  $T_{\text{p}}$ , the hardware turnaround delay from the reception state to the transmission state  $T_{\text{r2t}}$ , and the time required to transmit a packet  $T_{\text{tx}}$  with the IEEE 802.15.4 radio.  $T_{\text{slot}}$  can thus be calculated as

$$T_{\text{slot}} = T_{\text{sw}} + T_{\text{d}} + T_{\text{p}} + T_{\text{r2t}} + T_{\text{tx}}. \quad (10)$$

We define  $\tau_e$  as the time uncertainty during the time-slot  $T_{\text{slot}}$  in each hop. In CIBF,  $\tau_e$  accounts for the statistical uncertainty of the software delay  $\tau_{\text{sw}}$ , the radio processing uncertainty  $\tau_{\text{d}}$ , and the clock drift  $\tau_{\text{dr}}$  due to clock frequency drifts during the packet transmission. Therefore,  $\tau_e$  can be calculated as

$$\tau_e = \tau_{\text{sw}} + \tau_{\text{d}} + \tau_{\text{dr}}. \quad (11)$$


 Fig. 6.  $\Delta$  accumulates in a multihop worst-case topology.

Clock drift  $\tau_{\text{dr}}$  during a time-slot is caused by the oscillator frequency drifts of CC2420 radio. The low-cost oscillators always have a low aging factor (e.g.,  $\pm 3$  ppm/year) and a small temperature coefficient (e.g.,  $\pm 0.035$  ppm/ $^{\circ}$ C $^2$ ) [15]. We use the Gaussian random walk model [15], which characterizes the frequency drift  $\rho(t)$  relative to the nominal frequency  $f_0$  as a Gaussian random process with distribution  $N(0, \delta_{\rho}^2)$ . Since  $\rho(t)$  drifts slowly, it is reasonable to consider  $\rho(t)$  as a constant (denoted as  $\rho$ ) during the time-slot  $T_{\text{slot}}$ . Therefore, the clock drift  $\tau_{\text{dr}}$  due to oscillator frequency drifts is  $\tau_{\text{dr}} = \int_0^{T_{\text{slot}}} \rho(t) dt \approx \rho T_{\text{slot}}$ . The probability mass function (pmf)  $p_e$  of the time uncertainty  $\tau_e$  per hop is calculated as the convolution of the pmfs of the aforementioned independent random variables  $p_e = p_{\text{sw}} * p_{\text{d}} * p_{\text{dr}}$ , where  $p_{\text{sw}}$ ,  $p_{\text{d}}$ , and  $p_{\text{dr}}$  represent the pmfs of  $\tau_{\text{sw}}$ ,  $\tau_{\text{d}}$ , and  $\tau_{\text{dr}}$ , respectively. The pmf  $p_{\text{sw}}$  is determined by the software routine and the aforementioned two asynchronous clocks.  $\tau_{\text{sw}}$  is discrete distributed with time interval  $1/f_r$ , and we use the pmf  $p_{\text{sw}}$  measured with logical analyzer in [9]. For  $p_{\text{d}}$ , we introduce a granularity factor  $\kappa$  to discretize  $\tau_{\text{d}}$ , so that  $\kappa = 1/(m \cdot f_r)$ ,  $m \gg 1$ . Consequently,  $\tau_{\text{d}}$  has uniform discrete distribution  $\tau_{\text{d}} = \{0, \kappa, 2\kappa, \dots, 1/f_r\}$ , and  $p_{\text{d}}$  equals to  $1/(m + 1)$ . For  $p_{\text{dr}}$ , since  $p_{\text{dr}}$  is a Gaussian distributed variable, we intercept  $6\delta_{\rho} T_{\text{slot}}$  as the maximum value of  $\tau_{\text{dr}}$ , which covers 99.99% probability of all possible values. We discretize  $p_{\text{dr}}$  with time interval  $\varepsilon = 6\delta_{\rho} T_{\text{slot}}/m$ ,  $m \gg 1$ . As a result,  $\tau_{\text{dr}}$  has discrete distribution  $\tau_{\text{dr}} = \{-6\delta_{\rho} T_{\text{slot}}, \dots, 0, \varepsilon, 2\varepsilon, \dots, 6\delta_{\rho} T_{\text{slot}}\}$ , and  $p_{\text{dr}}(l\varepsilon)$  is calculated as

$$\begin{cases} \int_{l\varepsilon}^{(l+1)\varepsilon} \frac{1}{\delta_{\rho}\sqrt{2\pi}} e^{-\frac{x^2}{2\delta_{\rho}^2}} dx, & \text{when } l = -m + 1, \dots, m - 1 \\ \int_{-\infty}^{-(m-1)\varepsilon} \frac{1}{\delta_{\rho}\sqrt{2\pi}} e^{-\frac{x^2}{2\delta_{\rho}^2}} dx, & \text{when } l = -m, m. \end{cases} \quad (12)$$

A worst-case topology for CIBF is illustrated in Fig. 6. The sink node floods packets across  $m$  independent paths, each of which includes  $h$  hops. The  $m$  independent paths join again at a common receiver  $R_w$ . Let  $\Delta_m^h$  denote the maximum time displacement of  $m$  concurrent transmissions after  $h$  hops. Since the time uncertainty  $\tau_e$  accumulates after multihop packet receptions and retransmissions, at the common receiver,  $\Delta_m^h$  is likely to exceed the threshold period  $T_c$ , giving rise to collisions. Meanwhile, the growth of the number  $m$  of concurrent transmitters also increases the probability, with which  $\Delta_m^h$  exceeds the threshold period  $T_c$ . As the density or the size of a

wireless network grows, the precondition  $\Delta \leq T_c$  might not hold, thus incurring packet collisions.

For a path with  $h$  hops, let  $\tau_e^h$  denote the time uncertainty, and we have  $\tau_e^h = \sum_h \tau_e$ . The pmf  $p_e^h$  of accumulated time uncertainty  $\tau_e^h$  can be obtained by

$$p_e^h = \overbrace{p_e * \dots * p_e}^h. \quad (13)$$

The cumulative distribution function (CDF) of  $p_e^h$  is defined as

$$\begin{aligned} C_e^h(w) &\triangleq \sum_{\tau_e^h \leq w} p_e^h(\tau_e^h) \\ C_e^h(w-) &\triangleq \sum_{\tau_e^h < w} p_e^h(\tau_e^h). \end{aligned} \quad (14)$$

Therefore, the maximum temporal displacement  $\Delta_m^h$  at the common receiver  $R1$  is defined as the range of  $m$  independent identically distributed (i.i.d.) random variables, with distribution being equal to  $p_e^h$ . Consequently,  $\Delta_m^h$  can be calculated as

$$\Delta_m^h \triangleq \max(\tau_e^h(i)) - \min(\tau_e^h(j)), \quad 1 \leq i, j \leq m. \quad (15)$$

It can be formulated as an order statistics problem [16], and the pmf  $p_\Delta$  of temporal displacement  $\Delta_m^h$  is derived as

$$\begin{aligned} p_\Delta(\Delta_m^h = 0) &= \sum_{\tau_e^h} p_e^h(\tau_e^h)^m \\ p_\Delta(\Delta_m^h = w) &= \sum_{\tau_e^h} \left\{ [C_e^h(\tau_e^h + w) - C_e^h(\tau_e^h -)]^m \right. \\ &\quad - [C_e^h(\tau_e^h + w) - C_e^h(\tau_e^h)]^m \\ &\quad - [C_e^h(\tau_e^h + w-) - C_e^h(\tau_e^h -)]^m \\ &\quad \left. + [C_e^h(\tau_e^h + w-) - C_e^h(\tau_e^h)]^m \right\} \\ &\quad (w > 0). \end{aligned} \quad (16)$$

If we assume that each receiver can correctly decode the packet if it is in the communication radius of the transmitter and the possibility that correct packet receptions under destructive interference is 0, the PRR at node  $R1$  can be obtained by<sup>2</sup>

$$\text{PRR}_{R1}^{\text{Topo}} = C_\Delta(\Delta_m^h \leq 0.5\mu\text{s}) = \sum_{\Delta_m^h \leq 0.5} p_\Delta(\Delta_m^h). \quad (17)$$

We define retransmission times  $N$  as the maximum number of times a node transmits the same packet during a flooding process. Nodes can transmit a packet multiple times to increase the reception of correct packets. Corrupted packets might be caused by unreliable wireless links or unsynchronized transmissions resulting from temporal displacement accumulations. Therefore, recalling (9), we have the closed-form PRR formula

$$\text{PRR}_{R1} = 1 - (1 - \text{PRR}_{R1}^{\text{Topo}} \times \text{PRR}_{R1}^{\text{Link}})^N. \quad (18)$$

Testbed experiments show that average PRR during network flooding can approach 99% when  $N = 5$ [9]. In terms of PRR, CIBF is a highly reliable flooding protocol, although it provides no guarantee of delivering every packet successfully.

<sup>2</sup>From now on, we omit  $\mu\text{s}$  for simplicity when no confusion rises.

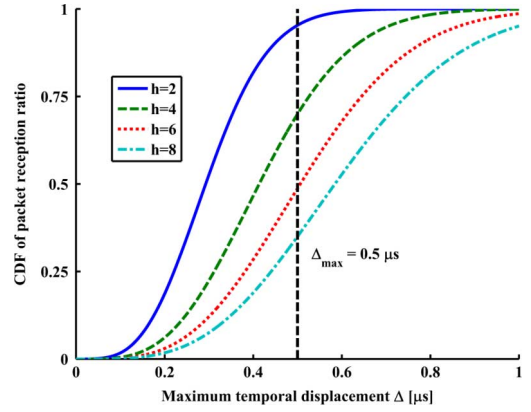


Fig. 7. CDF of PRR of  $R1$  versus  $\Delta_m^h$  of different  $h$  ( $m = 5$ ).

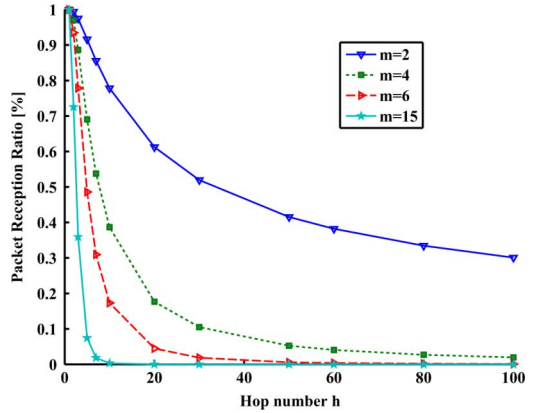


Fig. 8. PRR of  $R1$  versus hop number  $h$  with different  $m$ .

Fig. 7 illustrates the CDF of the maximum temporal displacement  $\Delta_m^h$  with different sizes  $h$  in the worst-case topology. We choose system settings of packet length 32 and clock frequency drift variance  $\delta_\rho = 5$  ppm. From Fig. 7, it can be observed that the CDF with  $m = 5, h = 6$  is only 50%, which is intolerable for system design, not to mention the size or the density of the network increases. Fig. 8 shows the PRR of  $R1$  versus the hop number  $h$  with different concurrent paths number  $m$ . It can be observed that the PRR of  $R1$  degrades significantly as the density or the size of the network increases. Indeed, we have the following lemma, which theoretically shows that the CIBF framework suffers the scalability problem.

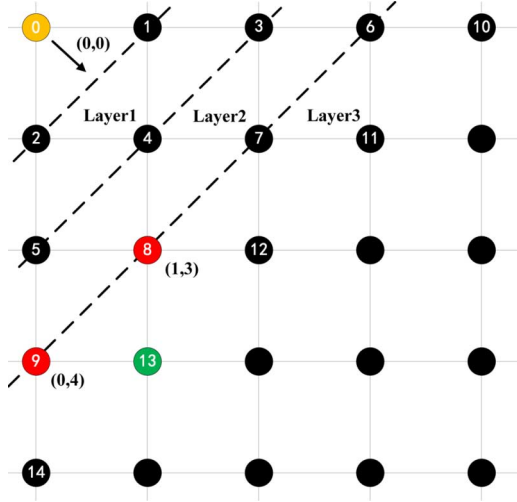
**Lemma 3.2:** when  $m \rightarrow \infty$  or  $h \rightarrow \infty$ , the PRR of node  $R1$  approaches 0.

Lemma 3.2 indicates that CIBF suffers the scalability problem, which should be addressed.

#### IV. SCALABLE FLOODING WITH NODE SELECTION

##### A. CIBF in Grid Networks

The aforementioned theoretical analysis provides a hint that the disclosed scalability problem has an intimate relationship with the network topology. To address this problem, network flooding in the grid topology is first analyzed as a special case. To help explain the packet propagation process, we use the term “slave” to stand for a receiver node. Since a slave node might have multiple parent transmitter nodes, we use the term “master” to represent the transmitter node dispatching the

Fig. 9. CIBF in a  $4 \times 4$  grid topology.

packet at the earliest time, while the term ‘‘assistant’’ denotes a concurrent transmission node, improving the packet reception. We make two general assumptions. First, the moment when a slave receives a packet is determined by its master. Second, since a slave has at most two parent transmitter nodes in a network with grid topology, the possibility for either parent transmitter becomes a master is  $1/2$ . Let  $T_1$  and  $T_2$  be the traversal times of a packet from the sink node to its two parents nodes  $N_1$  and  $N_2$ , respectively. Let  $p_{T_1}$  and  $p_{T_2}$  be the pmfs of arrival times  $T_1$  and  $T_2$ . In the unbounded grid topology, two parents nodes  $N_1$  and  $N_2$  are always symmetrical on the line connecting the sink node  $S$  and the slave node  $R$ . Thus, we have  $p(T_1 \leq T_2) = p(T_1 \geq T_2) = 0.5$ .

Fig. 9 illustrates CIBF in a simple  $4 \times 4$  grid topology. At first, the sink node  $N_0$  broadcasts a packet to one-hop slave nodes  $N_1$  and  $N_2$  at layer 1. After nodes  $N_1$  and  $N_2$  successfully receive the packet, they forward the packet immediately and simultaneously to nodes at layer 2, and so on and so forth. Considering node 13, its PRR equals to the CDF of maximum temporal displacement of packet transmissions between its parent transmitter nodes  $N_8$  and  $N_9$ . Notice that, throughout this paper, we do not consider successful packet receptions due to destructive interference. We also do not study packet collisions due to bursty links and node failures such as receiver queue overflow, packets duplicate suppression, task failure of operating systems, etc. Slave node  $N_8$  also has two parents  $N_4$  and  $N_5$ , each of which has  $1/2$  possibility to become the master of  $N_8$ . If node  $N_5$  becomes the slave node  $N_8$ 's master, nodes  $N_8$  and  $N_9$  have the same master  $N_5$ , which forms the two-hops independent path  $N_5 \rightarrow \{N_8, N_9\} \rightarrow N_{13}$ . With similar analysis, we can also obtain the three-hops independent path  $N_2 \rightarrow \{N_4, N_5\} \rightarrow \{N_8, N_9\} \rightarrow N_{13}$  and the four-hops independent path  $N_0 \rightarrow \{N_1, N_2\} \rightarrow \{N_4, N_5\} \rightarrow \{N_8, N_9\} \rightarrow N_{13}$ . The three independent paths cover all the circumstances that a common ancestor node floods a packet to node  $N_{13}$  through its parent nodes  $N_8$  and  $N_9$ . Consequently, the CDF of the maximum temporal displacement  $\Delta \leq 0.5 \mu\text{s}$  between  $N_8$  and  $N_9$  equals to the summation of the CDF in each independent case. To write simply, we define  $\Gamma_m^h(t) \triangleq C_{\Delta}^h(\Delta_m^h \leq t)$ . Thus,  $\Gamma_m^h(t)$  is the CDF of the maximum time displacement

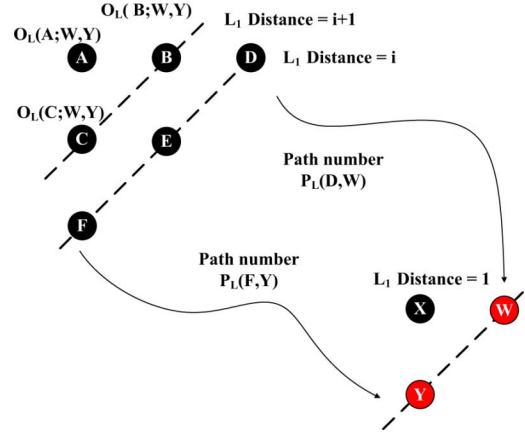


Fig. 10. CIBF in unbounded grid topology: nearby nodes dominate.

$\Delta_m^h$  of a common ancestor node propagating a packet along  $m$  concurrent paths with  $h$  hops. Therefore, according to the closed-form formula (17) and with the same parameter settings as in Section III-B, the PRR of node 13 can be acquired as

$$\begin{aligned} \text{PRR}_{13} = \Gamma(0.5)_{13} &= \frac{1}{2}\Gamma_2^2(0.5) \\ &+ \frac{1}{4}\Gamma_2^3(0.5) + \frac{1}{4}\Gamma_2^4(0.5) \\ &\approx 97.75\%. \end{aligned} \quad (19)$$

The following analysis calculates the packet reception performance for a node far away from the sink node. Without loss of generality, an unbounded grid topology is considered, and a representative pair of nodes  $N_W$  and  $N_Y$  is selected, as illustrated in Fig. 10.

To begin with, we define the  $L_1$ (Manhattan) distance,  $d_1^2$ , which is the summation of the lengths of the projections of the line segment between the points onto the coordinate axes in 2-D. For any path starting from the node  $P$  to the node  $Q$  along the edges in a grid network, the path is named as an  $L_1$  path of nodes  $P$  and  $Q$  (expressed by  $\chi_L(P, Q)$ ), if the length of the path equals to Manhattan distance  $d_1^2(P, Q)$ . If two  $L_1$  paths have no intersects in between (except for the end nodes), they are called a *disjoint*  $L_1$  path pair. The number of  $L_1$  paths between nodes  $P$  and  $Q$  is defined as  $P_L(P, Q)$ . The number of disjoint  $L_1$  path pairs from the node  $P$  to the node  $Q$  and the node  $R$  to the node  $S$  is denoted as  $O_L(P, R; Q, S)$ . If the node  $P$  and the node  $R$  are the same node,  $O_L(P; Q, S)$  is defined as the number of disjoint  $L_1$  path pairs belonging to the node  $P$ . The following lemmas hold.

**Lemma 4.1:** In Fig. 10, if  $d_1^2(A, Y) = d_1^2(A, W)$ , the number  $O_L(A; W, Y)$  of disjoint pairs from node  $N_A$  to nodes  $N_W$  and  $N_Y$  satisfies

$$1 \leq \frac{O_L(A; W, Y)}{O_L(B; W, Y) + O_L(C; W, Y)} \leq \frac{3}{2}. \quad (20)$$

**Lemma 4.2:** The layer  $i + 1$  is defined as follows: For any node  $P$  at layer  $i + 1$ , the  $L_1$  distance satisfies  $d_1^2(P, W) = d_1^2(P, Y) = i + 1$ . Let  $\Phi^{i+1}(W, Y)$  represent the aggregated probability that nodes  $W$  and  $Y$  receive a packet from all possible common ancestors at layer  $i + 1$ , we have  $\Phi^{i+1}(W, Y) \leq \frac{3}{4}\Phi^i(W, Y)$ .

*Lemma 4.3:* Let  $h_R$  be the hop number between the sink node  $S$  and the node  $R$  in a grid topology. For CIBF with the IEEE 802.15.4 radio, when  $h_R \rightarrow \infty$ , the expected PRR of  $R$  has a lower bound 94.5%.

Lemma 4.3 indicates that for CIBF in a grid topology, the PRR of a remote node has a lower bound (e.g., 94.5%) of successful packet reception. Generally speaking, nodes near the sink node have better PRR performance than that of remote nodes due to the time uncertainty  $\tau_m^h$  accumulating along multihop transmissions. Therefore, we can approximately consider that CIBF in a grid topology has high PRR performance even when the network scales.

Lemma 4.3 provides some key insights that the performance of CIBF has a close relationship with network topologies. First, common parent nodes can efficiently alleviate the accumulation of time displacements, which can reduce possible packet collisions in CIBF. Although the time displacements of packets from remote common ancestors might accumulate along the flooding paths, they are eliminated by common intermediate relaying nodes. Second, nearby parent nodes play a key role in the successful reception of a flooding packet. In the grid topology, a successfully received packet is much more probable from nearby parent nodes. Although remote common ancestors have more disjoint path pairs to the destination, those disjoint path pairs have lower probability to be chosen. Therefore, the total contribution for packet reception performance from remote common ancestors is low. Third, for CIBF, packet propagations paths should interleave each other if possible. Multiple independent propagation paths with long hops should be avoided to reduce time displacement accumulation.

### B. SCIF Protocol

The previously proposed CIBF algorithm such as Glossy is a topology-independent network flooding protocol. Glossy does not require each node to maintain the network-state information and can quickly adapt to node mobilities. However, as pointed out in the above analysis and experimented in real-world deployments, Glossy has the scalability problem and can only be applied in small-size networks. This drawback greatly limits the popularization of Glossy protocol in today's large-scale wireless network applications. For example, the performance is unacceptable when we apply Glossy for our *CitySee* project [17], which envisions to deploy thousands of wireless sensor nodes in an urban area of Wuxi City, China, such that multidimensional data including CO<sub>2</sub>, temperature, humidity, light, location, etc., could be collected in a real-time manner for environmental analysis. In the *CitySee* project, more than 4000 nodes are intended to be placed in a 20-km<sup>2</sup> urban area, forming a large-scale multihop wireless network with at least 20 hops. Once deployment, the network topology does not change frequently. This feature enables us to implement topology control algorithms in a centralized way and inject the obtained results into the sensor node before deployment.

Motivated by the *CitySee* project, we further propose SCIF, a CIBF protocol that is mainly applied in large-scale wireless networks with stable topology. In our scenario, it is reasonable to use the unit disk graph (UDG) to model the wireless network and assume the geographical locations of all nodes are known *a priori*. We first construct a spine of a given topology through

Algorithm 1. We then implement network flooding on the spine in the same way as Glossy. Different from Glossy, if the nodes do not belong to the spine, SCIF requires them only to receive the packets and keep silent, without retransmitting them again. To construct the grid spine, we divide the deployment area into several grid cells, with cell length  $1/\sqrt{5}$  of the communication radius  $R$ . Therefore, two arbitrary nodes can have an edge if they belong to adjacent cells. With the proposed spine construction method, a virtual grid backbone is constructed, on which CIBF has been shown to be scalable as the density or the size of the network scales (Lemma 4.3). Since a spine node might overhear flooding packets from other cells, it only forwards packets when its hop number  $H_i$  matches the relay counter  $c$  in the packet. In this way, SCIF ensures that overheard packets do not destroy the rhythm of the whole flooding process. After each successful packet reception, the ordinary dominantes keep silent or enter the sleep state to save energy, without forwarding the packet. The pseudocode of SCIF is described in Algorithm 2.

---

#### Algorithm 1: Spine Construction

---

**Input:** Given a node set  $\Phi < ID_i, X_i, Y_i >$ , a sink node  $< 0, 0, 0 >$ , communication radius  $R$   
**Output:** A spine set  $\Omega < bS_i, H_i >$ , where  $bS_i$  denotes whether a node  $i$  belongs to the spine, and  $H_i$  represents the minimum hop number from the sink node. For nonspine node,  $H_i = 0$ .

- 1 Project each node on the  $x$ - and  $y$ -axes and acquire the cell each node belongs to;
- 2 For nodes in the same cell, let the node  $j$  with the minimum ID as a spine node ( $bS_j = 1$ );
- 3 Construct graph  $G(V, E)$  with all spine nodes. Two nodes can have an edge only if they belong to adjacent cells;
- 4 Search the graph  $G(V, E)$  using BFS algorithm;
- 5 **if** *More than one tree is created* **then**
- 6     constructed spine is not connected graph, return **false**;
- 7 **else**
- 8     let  $H_i$  be the hop number a spine node from the sink node
- 9     return **true**;
- 10 **end**
- 11 **end**

---



---

#### Algorithm 2: SCIF

---

**Input :** For each node, given spine attributes  $< bS_i, H_i >$

- 1 Whenever a node receives a packet  $P$ , it stores it and decodes relay counter  $c$  from the packet  $P$ ;
- 2 **if** *the node is a spine node* ( $bS_i = 1$ ) **then**
- 3     **if**  $c = H_i$ , *indicating the very packet to forward* **then**
- 4         increase the relay counter  $c$  by 1, and forward the packet  $P$  immediately;
- 5     **else**
- 6         delete packet  $P$  for it is an overheard packet;
- 7     **end**
- 8 **end**
- 9 **end**

---

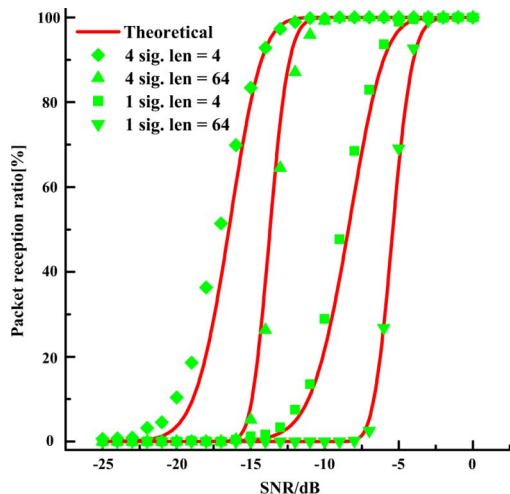


Fig. 11. PRR versus SNR for 802.15.4 radio without CI.

*Time Complexity:* We will provide time complexity analysis of the centralized spine construction algorithm. In Algorithm 1, the first step takes an  $O(n)$  time complexity. The second step selects the minimum number in a number set, which costs an  $O(n)$  time. To test connectivity of the spine nodes, we first construct a graph  $G(V, E)$ , and then traverse the graph with the BFS algorithm. The two steps have an  $O(n^2)$  time complexity. Therefore, the overall time complexity of the spine construction algorithm is  $O(n^2)$ .

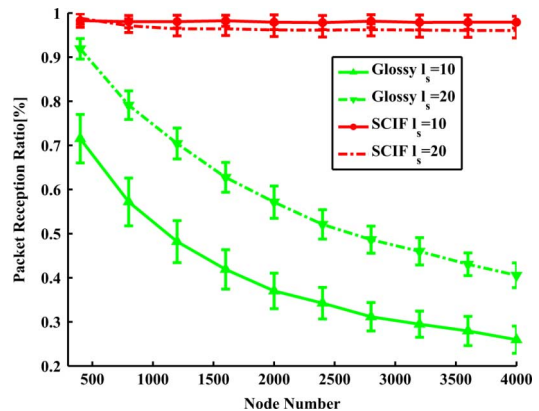
## V. SIMULATIONS

### A. Validation of Closed-Form PRR Formula (9)

We simulate a simplified IEEE 802.15.4 radio framework to validate theoretical waveform analysis, and the results are shown in Fig. 11. An original signal and three replicas, which have relative amplitudes  $[1 \ 0.5 \ 1.5]$  and phase offsets  $[0.25 \ 0.5 \ 0.75]T_c$ , are superposed to a common receiver. Packets with length 4 and 64 are used to verify the performance of different system settings. To show the contribution of CI, the original signal without any replica is also simulated. All simulation results are averaged by 1000 times to compare to theoretical results obtained by (6) and (9). From Fig. 11, it can be observed that curves generated by theoretical analysis matches with the simulation results very well. Therefore, simulation results validate the correctness of the closed-form formula (9). For both settings of transmission packet lengths 4 and 64, the measured IGF values are about 9 dB, equaling to that obtained by (6). It indicates that the performance gain of CI is determined by relative amplitudes and phase offsets of replicas with the original signal. Furthermore, both the theoretical analysis and simulation results show that packets of longer length are much more easily corrupted by external interferences.

### B. Performance Evaluation of SCIF

To evaluate the effectiveness of the proposed SCIF protocol, we run extensive simulations both in large-scale uniformly distributed networks and the topology of the CitySee project

Fig. 12. PRR versus node number  $N_s$ .

with real data trace.<sup>3</sup> We compare the packet reception performance of SCIF to that of Glossy. For the uniformly distributed topology, nodes are randomly deployed in a square area, with the number  $N_s$  varying from 400 to 4000 with a step of 400. The communication radius  $R$  of a transmitter is fixed as 2, the edge length of each grid cell is 1 and the length of the square area  $l_s$  varies from 5 to 40 with a step of 5.

We vary the communication radius  $R$  from 1.2 to 4 with a step of 0.4 and assign the cell edge  $R/\sqrt{5}$ . For the fairness of the comparison, both protocols use the same theoretical model proposed in Section III-B. We suppose that all nodes use omnidirectional antennas and have the same transmission range. We also assume that a broadcast packet can be received by nodes that are within the communication radius of the transmitter. Other system parameters include: the length of packet payload 32, the variance of clock frequency drift  $\delta_\rho = 5$  ppm, the threshold of time displacement  $T_c = 0.5 \mu\text{s}$  (for the IEEE 802.15.4 radio), the retransmission times  $N = 1$ , and the period during one-hop packet reception and retransmission  $T_{\text{slot}} = 1.124$  ms. Simulation results are averaged by 100 times and are implemented on the MATLAB 7.11 platform.

For the uniformly distributed topology, Figs. 12 and 13 show the PRR performance as the density and the size of the network vary. From Figs. 12 and 13, it can be observed that SCIF outperforms Glossy in terms of PRR. The PRR performance of Glossy is significantly influenced by the network density or network size, while that of SCIF keeps nearly constant. The simulation evaluations indicate that CIBF with SCIF is more scalable than Glossy. Fig. 12 illustrates PRR versus node number  $N_s$  with square area lengths  $l_s = 10$  and  $l_s = 20$ . Particularly, when  $N_s = 4000$  and  $l_s = 10$ , the PRR value of Glossy is 26%, while the PRR value of SCIF is 97%. Fig. 13 shows that the situation of PRR versus  $l_s$  with fixed node numbers  $N_s = 1000$  and  $N_s = 4000$ . Although the reception performance of SCIF decreases as the size of the network grows, its PRR value is higher than 96% (bounded by Lemma 4.3, 94.5%).

Fig. 14 depicts the overall flooding latency in each experiment setting as the size of the network varies. It can be observed that the increase of PRR performance of SCIF is at the cost of sacrificing flooding latency. When  $N_s = 4000$ , the average flooding latency of SCIF is almost  $2.5\times$  that of Glossy. When

<sup>3</sup>Detailed trace driven simulation results are provided in [14].

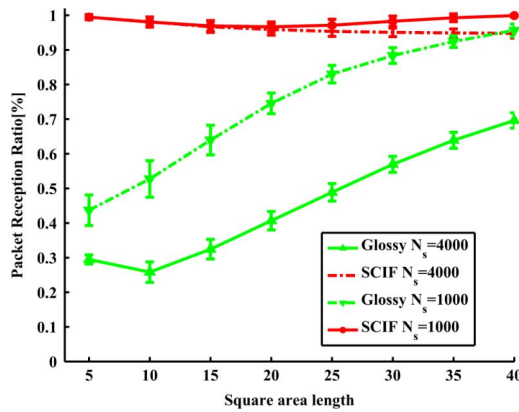


Fig. 13. PRR versus square area length  $l_s$ .

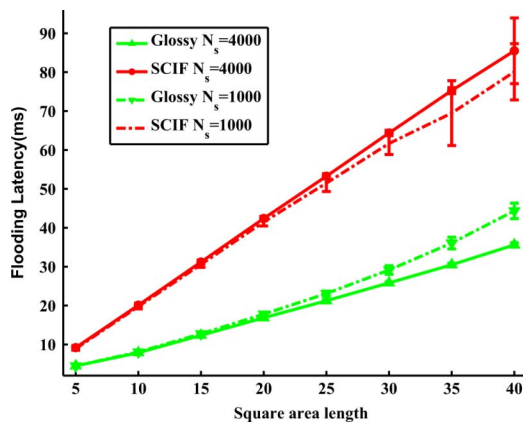


Fig. 14. Flooding latency versus square area length  $l_s$ .

$N_s = 1000$ , the average flooding latency of SCIF is almost  $1.8 \times$  that of Glossy. Since Glossy is a latency-optimal flooding protocol, and experiments have shown that network flooding of Glossy normally takes up a magnitude of milliseconds [9], this cost is rather worthwhile.

## VI. RELATED WORK

Exploiting concurrent transmissions over interference in wireless networks is a promising trend, for its ability to increase network throughput[18], to alleviate the broadcast storm problem of acknowledgments[11], to enhance packet transmission reliability[19], and to reduce flooding latency [8]. Prior works can be categorized as signal-processing-based and physical-layer-phenomenon-based. Signal-processing-based works leverage powerful software-defined radio platforms (e.g., USRP), including ANC[20] for network coding, SIC [21] for interference cancellation, multiple-input-multiple-output (MIMO) interference alignment and cancellation[22], etc.

Physical-layer-phenomenon-based works mainly focus on exploring wireless radio properties such as the capture effect [7] and message-in-message (MIM) [21], both of which do not require nodes to concurrently transmit the same packet. However, techniques leveraging the capture effect or the MIM physical phenomena either require the strong signal arriving first or need special hardware support to continuously search for the stronger signal. Differing from the capture effect and MIM, CI stems from the physical-layer tolerance for multipath

signals. CI is experimentally discovered by Dutta *et al.* [23], who explore concurrent transmissions of short acknowledgment packets automatically generated by the radio hardware, to alleviate the ACK implosion problem [11].

The proposed SCIF protocol is related to prior work on network flooding, which is a fundamental service in wireless networks. Previous works like CF [4] and RBP [6] improve network flooding performance by leveraging link characteristics and identifying which nodes to relay packets. Opportunistic flooding [5] can efficiently reduce flooding latency and redundancy by using links outside the energy optimal tree to forward opportunistically early packets. Those protocols [4]–[6] require nodes to maintain the working states of nearby neighbors, introducing huge overhead. Moreover, they rely on the CSMA/CA protocol for MAC-layer access and collision avoidance, while SCIF exploits CI, which increases network concurrency and thus greatly reduces flooding latency. By exploring the capture effect and utilizing controlled concurrency techniques, Flash [8] can realize rapid network flooding with 2 s latency for 90% reliability. Flash requires the stringent power control to guarantee PRR and the flooding performance degrades significantly as the density or the size of the network increases. SCIF can also benefit from the capture effect. The difference between them is that concurrent transmissions in FLASH are not synchronized as accurately as SCIF, which cause excessive packet collisions when the network becomes dense. By implementing elaborate designs such as the compensation of MCU irregular instructions and the disablement of irrelevant interrupts as well as hardware timers, Glossy [9] realizes precise timing to control multiple senders to transmit packets simultaneously. Therefore, Glossy employs CI to achieve a magnitude of millisecond flooding latency of data (not acknowledgment). Nevertheless, as disclosed in this paper, Glossy suffers the scalability problem, namely, the PRR performance of Glossy degrades significantly as the density or the size of the network increases. The main objective of SCIF is to address this problem.

Our design SCIF is also related to prior work on topology control. There are a number of examples that utilize topology control to realize efficient routing in wireless networks [24]. The most common techniques of topology control are locally constructing connected dominating set (CDS). SCIF proposes a lightweight approach to construct the spine of a network. Being approximately considered as a grid topology, the spine structure is shown to be able to efficiently resist packet collisions due to scalable flooding with CI. SCIF adopts the proposed lightweight topology control method to solve the scalability problem.

## VII. CONCLUSION

CIBF is a nascent trend due to its ability to realize near-optimal network flooding latency and submicrosecond time synchronization accuracy. With waveform analysis, we examine the root cause of CI, which is previously observed only in simulations and experiments. We derive the closed-form PRR formula and thoroughly reveal the scalability problem in CIBF through both theoretical analysis and extensive simulations. We show CIBF is scalable (PRR lower bound 94.5%) in the grid topology. Enlightened by this key insight, we further propose the SCIF protocol, which outperforms Glossy in terms of the PRR performance when the density or the size of the network

grows. Our future work includes the performance measurements of SCIF in real-world large-scale wireless sensor networks, the exploitation of CI in time synchronization, and application of CI in wireless remote reprogramming.

## REFERENCES

- [1] G. Tolle and D. Culler, "Design of an application-cooperative management system for wireless sensor networks," in *Proc. EWSN*, 2005, pp. 121–132.
- [2] M. Maròti, B. Kusy, G. Simon, and À. Lèdeczi, "The flooding time synchronization protocol," in *Proc. ACM SenSys*, 2004, pp. 39–49.
- [3] Z. Li, M. Li, J. Wang, and Z. Cao, "Ubiquitous data collection for mobile users in wireless sensor networks," in *Proc. IEEE INFOCOM*, 2011, pp. 2246–2254.
- [4] T. Zhu, Z. Zhong, T. He, and Z. Zhang, "Exploring link correlation for efficient flooding in wireless sensor networks," in *Proc. USENIX NSDI*, 2010, pp. 49–63.
- [5] S. Guo, Y. Gu, B. Jiang, and T. He, "Opportunistic flooding in low-duty-cycle wireless sensor networks with unreliable links," in *Proc. ACM MobiCom*, 2010, pp. 133–144.
- [6] F. Stann, J. Heidemann, R. Shroff, and M. Murtaza, "RBP: robust broadcast propagation in wireless networks," in *Proc. ACM SenSys*, 2006, pp. 85–98.
- [7] K. Leentvaar and J. Flint, "The capture effect in FM receivers," *IEEE Trans. Commun.*, vol. COM-24, no. 5, pp. 531–539, May 1976.
- [8] J. Lu and K. Whitehouse, "Flash flooding: Exploiting the capture effect for rapid flooding in wireless sensor networks," in *Proc. IEEE INFOCOM*, 2009, pp. 2491–2499.
- [9] F. Ferrari, M. Zimmerling, L. Thiele, and O. Saukh, "Efficient network flooding and time synchronization with glossy," in *Proc. ACM/IEEE IPSN*, 2011, pp. 73–84.
- [10] P. Dutta, S. Dawson-Haggerty, Y. Chen, C. Liang, and A. Terzis, "Design and evaluation of a versatile and efficient receiver-initiated link layer for low-power wireless," in *Proc. ACM SenSys*, 2010, pp. 1–14.
- [11] S. Ni, Y. Tseng, Y. Chen, and J. Sheu, "The broadcast storm problem in a mobile ad hoc network," in *Proc. ACM MobiCom*, 1999, pp. 151–162.
- [12] H. Rahul, H. Hassanieh, and D. Katabi, "SourceSync: A distributed wireless architecture for exploiting sender diversity," in *Proc. ACM SIGCOMM*, 2010, pp. 171–182.
- [13] N. Oh and S. Lee, "Building a 2.4-GHz radio transceiver using IEEE 802.15.4," *IEEE Circuits Devices Mag.*, vol. 21, no. 6, pp. 43–51, Jan.–Feb. 2006.
- [14] Y. Wang, Y. He, X. Mao, Y. Liu, and X.-Y. Li, "Exploiting constructive interference for scalable flooding in wireless networks," 2012 [Online]. Available: <https://sites.google.com/site/ywangthu10/>
- [15] Z. Zhong, P. Chen, and T. He, "On-demand time synchronization with predictable accuracy," in *Proc. IEEE INFOCOM*, 2011, pp. 2480–2488.
- [16] B. Arnold, N. Balakrishnan, and H. Nagaraja, *A First Course in Order Statistics*. Philadelphia, PA, USA: SIAM, 2008.
- [17] X. Mao, X. Miao, Y. He, X.-Y. Li, and Y. Liu, "Citysee: Urban CO<sub>2</sub> monitoring with sensors," in *Proc. IEEE INFOCOM*, 2012, pp. 1611–1619.
- [18] X. Wang, W. Huang, S. Wang, J. Zhang, and C. Hu, "Delay and capacity tradeoff analysis for motioncast," *IEEE/ACM Trans. Netw.*, vol. 19, no. 5, pp. 1354–1367, Oct. 2011.
- [19] X. Wang, L. Fu, and C. Hu, "Multicast performance with hierarchical cooperation," *IEEE/ACM Trans. Netw.*, vol. 20, no. 3, pp. 917–930, Jun. 2010.
- [20] S. Katti, S. Gollakota, and D. Katabi, "Embracing wireless interference: Analog network coding," in *Proc. ACM SIGCOMM*, 2007, pp. 397–408.
- [21] D. Halperin, T. Anderson, and D. Wetherall, "Taking the sting out of carrier sense: interference cancellation for wireless LANs," in *Proc. ACM MobiCom*, 2008, pp. 339–350.
- [22] K. Lin, S. Gollakota, and D. Katabi, "Random access heterogeneous MIMO networks," in *Proc. ACM SIGCOMM*, 2011, pp. 146–157.
- [23] P. Dutta, R. Mualoiu-E, I. Stoica, and A. Terzis, "Wireless ACK collisions not considered harmful," in *Proc. ACM HotNets-VII*, 2008, pp. 19–24.
- [24] K. Alzoubi, P. Wan, and O. Frieder, "Message-optimal connected dominating sets in mobile ad hoc networks," in *Proc. ACM MobiHoc*, 2002, pp. 157–164.



**Yin Wang** (M'08) received the B.S. and M.S. degrees in electronic engineering from Tsinghua University, Beijing, China, in 2004 and 2007, respectively, and is currently pursuing the Ph.D. degree in computer science at Tsinghua University.

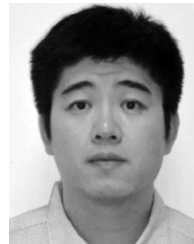
His research interests include wireless sensor networks, Internet of things, mobile computing, and distributed simulation.



**Yuan He** (M'07) received the B.S. degree in computer science from the University of Science and Technology of China, Hefei, China, in 2003, the M.S. degree in computer software and theory from the Chinese Academy of Sciences, Beijing, China, in 2006, and the Ph.D. degree in computer science and engineering from the Hong Kong University of Science and Technology, Hong Kong, in 2010.

He is a member of the Tsinghua National Lab for Information Science and Technology, Beijing, China.

His research interests include wireless and sensor networks, mobile computing, and peer-to-peer computing.



**Xufei Mao** (M'10) received the B.S. degree from Shenyang University of Technology, Shenyang, China, in 1999, the M.S. degree from Northeastern University, Boston, MA, USA, in 2003, and the Ph.D. degree from the Illinois Institute of Technology, Chicago, IL, USA, in 2010, all in computer science.

He is a member of the Tsinghua National Lab for Information Science and Technology, Beijing, China.

His research interests span wireless sensor networks, pervasive computing and mobile cloud computing.



**Yunhao Liu** (M'02–SM'06) received the B.S. degree in automation from Tsinghua University, Beijing, China, in 1995, and the M.S. and Ph.D. degrees in computer science and engineering from Michigan State University, East Lansing, MI, USA, in 2003 and 2004, respectively.

He is now the Cheung Kong Professor with Tsinghua University, as well as a faculty member with the Hong Kong University of Science and Technology, Hong Kong. His research interests include

wireless sensor networks, peer-to-peer computing, and pervasive computing.



**Xiang-yang Li** (M'99–SM'09) received the B.S. degree in computer science and the Bachelor's degree in business management from Tsinghua University, Beijing, China, both in 1995, and the M.S. and Ph.D. degrees in computer science from the University of Illinois at Urbana–Champaign, Urbana, IL, USA, in 2000 and 2001, respectively.

He is a Professor with the Illinois Institute of Technology, Chicago, IL, USA. His research interests include mobile computing, cyber-physical systems, wireless networks, security and privacy,

and algorithms.